Monatshefte für Chemie - Chemical Monthly
https://doi.org/10.1007/s00706-018-2244-5

ORIGINAL PAPER

Asymmetric synthesis and study of biological activity of (epi-) benzoanalogues of bioactive phenanthroquinolizidine alkaloids

Tomáš Pagáč[1] · Peter Šafář[2] · Štefan Marchalín[2] · Zuzana Ježíková[1] · Barbora Balónová[2] · Miroslava Šupolíková[3] · Eva Nováková[3] · Jana Kubíčková[1] · Michal Šoral[4] · Július Sivý[5] · Petra Olejníková[1]

Received: 17 March 2018 / Accepted: 23 May 2018

Abstract

The increasing microbial resistance to primary active structures remains alarming and the effort to look for new antibacterial active structures is still of scientific interest. One of the attractive ways to find new active structures is derivatization of well-known natural compounds. Alkaloids are a structurally diverse group of natural products with a wide range of biological effects. Historically, an attempt to increase the antimicrobial activity of alkaloids through chemical modifications has been successful. In this work, 12 new quinolizidine derivatives were synthesized and tested for their antimicrobial activity. The asymmetric synthesis of the benzoanalogue of the phenanthroquinolizidine bioactive alkaloid (−)-cryptopleurine and the epi-benzoanalogues of (−)-(15*R*)-hydroxycryptopleurine were achieved in six or seven steps starting from available enantiopure (*S*)-2-aminoadipic acid used as source of chirality as well as nitrogen. The highest antimicrobial activity was observed in the presence of the final saturated structure, the benzoanalogue of naturally occurring plant alkaloid cryptopleurine. It features selective toxicity, and significantly inhibits the growth of G^+ bacteria, especially *Staphylococcus* sp. Tested derivatives have shown only a weak antifungal activity, but partial inhibition has been observed in the case of model yeasts.

Graphical abstract

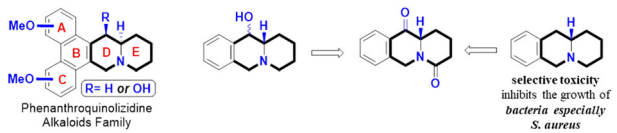

Keywords Antimicrobial activity · Benzoanalogue of the natural phenanthroquinolizidine bioactive alkaloids · Quinolizidine derivatives

Electronic supplementary material The online version of this article (https://doi.org/10.1007/s00706-018-2244-5) contains supplementary material, which is available to authorized users.

✉ Petra Olejníková
petra.olejnikova@gmail.com

[1] Institute of Biochemistry and Microbiology, Faculty of Chemical and Food Technology, Slovak University of Technology in Bratislava, 81237 Bratislava, Slovak Republic

[2] Department of Organic Chemistry, Faculty of Chemical and Food Technology, Slovak University of Technology in Bratislava, 81237 Bratislava, Slovak Republic

[3] Department of Microbiology and Virology, Faculty of Natural Sciences, Comenius University, 84215 Bratislava, Slovak Republic

[4] Central Laboratories, Faculty of Chemical and Food Technology, Slovak University of Technology in Bratislava, 81237 Bratislava, Slovak Republic

[5] Institute of Mathematics and Physics, Faculty of Mechanical Engineering, Slovak University of Technology in Bratislava, Námestie slobody 17, 812 31 Bratislava, Slovak Republic

Published online: 22 August 2018

Introduction

Efforts to discover new antibacterial active compounds are constantly growing, spurred by the development of microbial resistance. The development and increase in resistant microorganisms to the originally effective structures forces the scientists to look further for active compounds [1]. The current trend favors the derivatization of natural molecules by organic synthesis [2]. Alkaloids are a structurally diverse group of natural products with a wide range of biological effects [3]. Many naturally occurring plant alkaloid derivatives have shown wide spectra of biological properties, including cytotoxic, oxytocic, antipyretic, antibacterial, antiviral, and hypoglycemic activities, as determined by in vivo pharmacological screening [4]. Some of them are used in clinical treatment of diabetes [5] or they act as inhibitors of testosterone-5α-reductase, which is of great importance for treatment of various skin diseases, for example, acne treatment, as well as excessive hair loss treatment [6, 7]. An attempt to increase the antimicrobial activity of alkaloids by chemical modifications has been quite successful. Interesting biological activity has been achieved in compounds where the indole, isoquinoline, pyrrolide, and thiazole were used as pharmacophore [3]. Quinolizidines (QA), known as lupine alkaloids are rare, but their biological activity is well documented. In nature they originate from plants, mostly as secondary metabolites of *Lupinus*, *Leguminosaceae* [8] and are derived from the amino acid lysine (Lys) [4]. Lys is known as the precursor of piperidine, quinolizidine, indolizidine and lycopene alkaloids as compounds occurring in the plant kingdom. Natural QA alkaloids are synthesized by cyclization of the cadaverine unit and are further modified by adaptation reactions (e.g., dehydrogenation, oxygenation, or esterification) to give hundreds of structurally related alkaloids [9]. Synthetically prepared derivatives of natural lead structures possess interesting biological effects as well even negligible antimicrobial activity [10]. A number of synthetically prepared derivatives had been tested as antimycobacterial compounds for the potential treatment of tuberculosis [11]. An attempt to increase the antimicrobial activity of alkaloids by chemical modifications has been quite successful [2]. According to antimicrobial activity of quinolizidine structures they show greater efficacy on G^+ bacteria and mycobacteria [12]. Animal toxicity studies using CHO-K1 [13], HEK 293 [14], and VERO cells [12] suggest that the compounds have selective toxicity on prokaryotic cells. In this work, benzoanalogues and epi-benzoanalogues of bioactive phenanthroquinolizidine alkaloids (Fig. 1) were prepared by asymmetric synthesis and were tested for their potential antimicrobial activity (Scheme 1).

Results and discussion

The synthesis of the starting pyridoisoquinolinedione **4** comprises reductive amination of benzaldehyde with available (*S*)-2-aminoadipic acid (**1**), followed by an intramolecular *N*-acylation of the resulting *N*-benzyl aminoadipic acid **2** to the 6-oxopipecolinic acid **3** [15]. Finally, intramolecular Friedel–Crafts acylation afforded ketone **4** in 56% overall yield [16].

The diastereoselective reduction of the ketone **4** with $NaBH_4$ reflects a preference for an axial hydride attack from the more hindered *endo* face of the tricyclic system (Scheme 2). Thus, the reduction with $NaBH_4$ at 0 °C in methanol gave *trans*-**5a** in 73% yield. The stereoselectivity can be reversed using a bulkier hydride reagent that can block the hydride axial approach observed with $NaBH_4$. Reduction of ketone **4** with L-Selectride solution in THF at − 40 °C afforded alcohol *cis*-**5b** in 60% yield. The distributions of diastereomers **5a**, **5b** are in accordance with those obtained in our group's earlier investigations of indolizidindiones containing fused thiophene and benzothiophene rings [17–19] and thienoquinolizidindiones [20]. The stereochemical assignments of these alcohols are based on the analysis of the multiplet shapes of ^{1}H NMR signals of H11 and H11a. The $^3J_{11,11a}$ coupling constant value served as a reliable and readily available descriptor—its obvious difference for **5a** (9.7 Hz) and **5b** (1.6 Hz) reflected the, respectively, pseudoaxial–axial and pseudoequatorial–axial orientations of the abovementioned pair of hydrogens.

With the ultimate objective to prepare the enantiopure benzoanalogues **7** and **11** of the naturally occurring (−)-cryptopleurine and (−)-(15*R*)-hydroxycryptopleurine, the reduction of the lactam group and OH function to the corresponding alkane was envisioned.

In this perspective, alcohols *trans*-**5a** and *cis*-**5b** were acetylated using standard conditions (Scheme 2). Their reaction with acetic anhydride in the presence of dry triethylamine and catalytic amounts of DMAP in CH_2Cl_2 at room temperature led to the acetoxy derivatives *trans*-(11*R*,11a*S*)-**6a** and *cis*-(11*S*,11a*S*)-**6b** in yields of 70 and 75%, respectively. Ultimately, these acetyl derivatives *trans*-**6a** and *cis*-**6b** were efficiently converted into the expected benzoquinolizidinols *trans*-**7a** and *cis*-**7b** in good yields (71 and 76%) using LAH reduction in refluxing THF for 1 h according to Green's protocol developed during the stereoselective synthesis of the alkaloids (−)-2-epilentiginosine and (+)-lentiginosine [21].

The quaternization of basic epimeric alcohols **7a**, **7b** with CH_3I provide the corresponding benzoquinolizinium salts **8a**, **8b** in 78–81% yields. The relative configuration of compounds **8a**, **8b** was deduced from the observed NOE

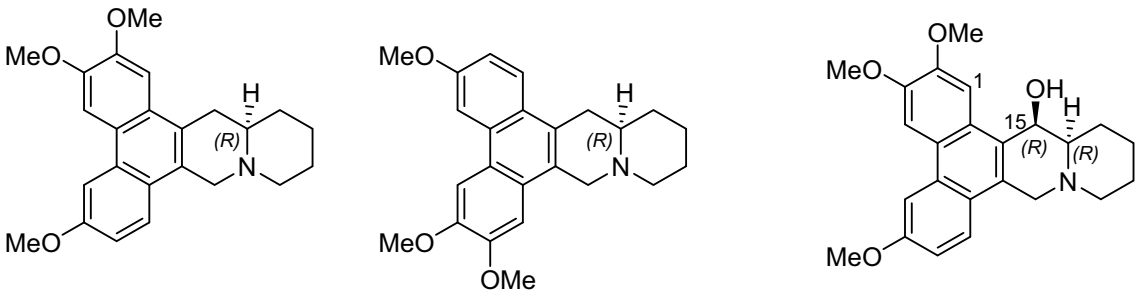

Fig. 1 Structures of representative natural phenanthroquinolizidine alkaloids

Scheme 1

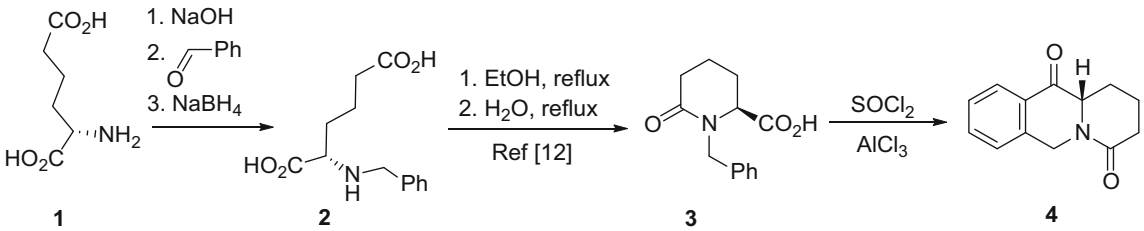

Scheme 2

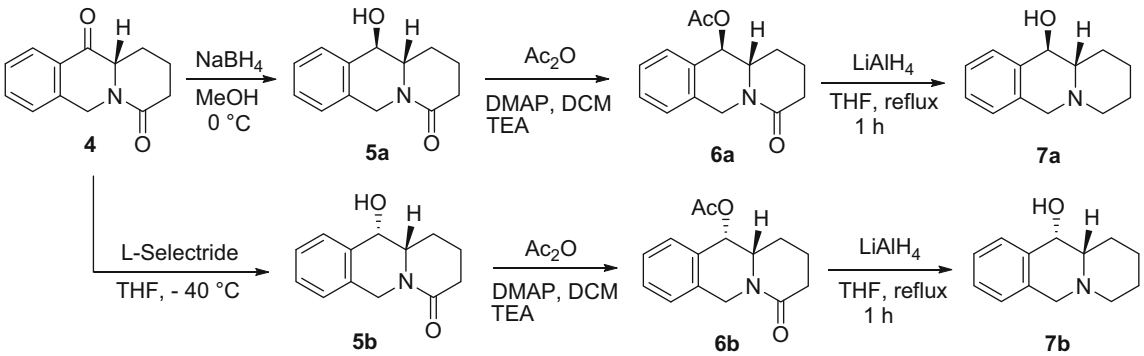

Scheme 3

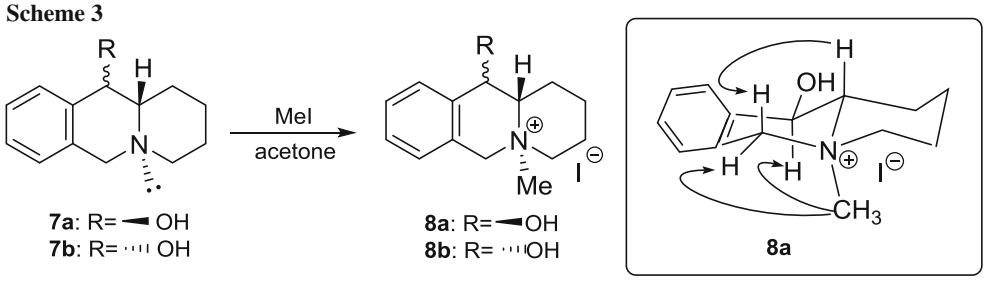

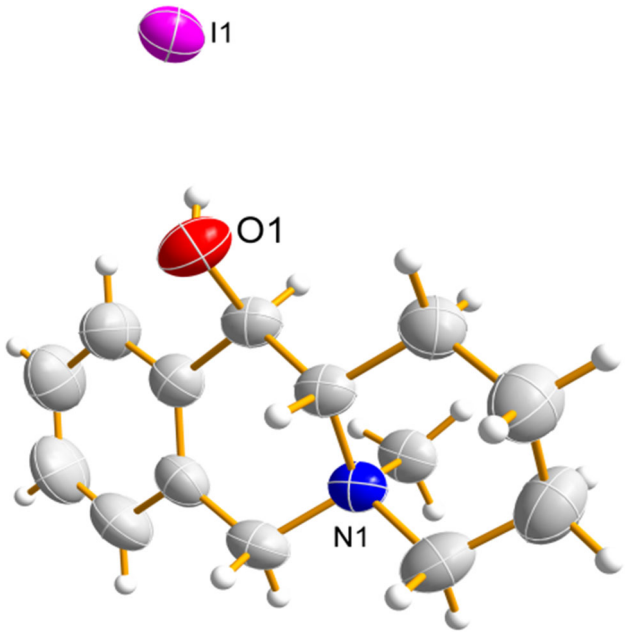

Fig. 2 ORTEP drawing of **8a**

enhancements in their 2D NOESY NMR spectra (Scheme 3) and was secured by X-ray crystallographic analysis of a single crystal of the methiodide salt *trans*-**8a** (Fig. 2).

Since attempts to remove the OH function from enantiopure alcohols **7a** or **7b** with triethylsilane in TFA failed to provide the targeted quinolizidinone **11** we turned our attention to the Barton–McCombie deoxygenation protocol. For this reason, alcohol *trans*-**5a** was converted to the corresponding xanthate (11*R*,11a*S*)-**9** in a yield of 81%.

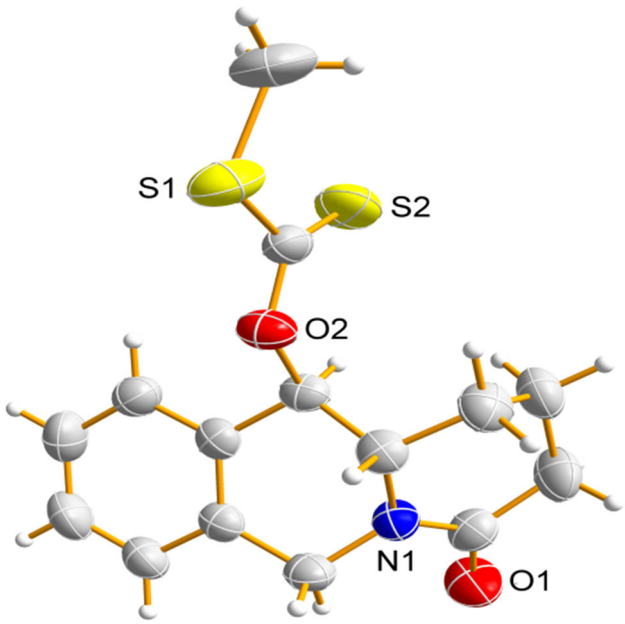

Fig. 3 ORTEP drawing of **9**

The structure of this compound was unambiguously confirmed by single crystal X-ray diffraction analysis (Fig. 3). The xanthate functionality was then reductively removed using Bu_3SnH in the presence of a catalytic amount of AIBN (toluene, reflux, 75%) forming the lactam **10**.

Finally, lactam **10** was directly converted to the targeted enantiopure (*S*)-2,3,4,6,11,11a-hexahydro-1*H*-pyrido[1,2-*b*]isoquinoline (**11**) using LAH reduction in refluxing THF for 1 h in a 79% yield after recrystallization from dry *i*-hexane (Scheme 4).

The newly synthesized set of derivatives within this study (Fig. 4) was tested for its antimicrobial activity in vitro using bacteria (*S. aureus*, MRSA isolates—SA21528, SAL18, *S. epidermidis*, *P. aeruginosa*, *E. coli*), yeasts (*C. albicans*, *C. parapsilosis*) and filamentous fungi (*F. culmorum*, *M. gypseum*, *T. terrestre*, *B. cinerea*, *A. alternata*). The highest antibacterial activity was reached in derivative **11** (benzoanalogue of cryptopleurine) and derivative **9**. These two derivatives were tested for their cytotoxicity on BHK-21 and VERO cells as well.

The best antibacterial properties were observed in the presence of derivative **11**. In the case of Gram-positive bacteria, derivative **11** was able to inhibit the growth of all *Staphylococcus* sp. used in this study (see Table 1); it was possible to obtain the MIC_{100} values for all tested strains of *Staphylococcus* sp. The highest sensitivity was observed for *S. aureus* at a concentration of 5 μg/cm^3 with bacteriostatic effect on the cells. In addition, derivative **9** was able to inhibit the growth of *S. aureus* but in higher concentration (100 μg/cm^3) when compared to derivative **11** (Table 1). As such an important antibacterial effect was detected on *S. aureus,* the growth inhibition of two hospital MRSA isolates was attempted. Derivative **11** was able to inhibit the growth of both isolates (MIC_{100} were detected) but in ten times higher concentration as was found for *S. aureus* CCM 3953 (Table 1), i.e., the MIC_{100} value was observed at the concentration of 50 μg/cm^3 for both isolates. Sensitivity of *S. epidermidis* was observed as well—its 100% growth inhibition in the presence of the derivative **11** was observed at the concentration of 10 μg/cm^3 with bacteriostatic effect on the cells.

Newly synthesized derivative **11** with the highest antibacterial activity was tested for its potential for biofilm eradication. The derivative was present in the medium throughout the biofilm formation of strain *S. epidermidis* CCM 7221 (recommended for biofilm assay). The effect of derivative **11** on biofilm formation was concentration dependent and is shown in Table 2. Significant decrease in biofilm formation was observed in the presence of derivative **11** at the concentration 10 and 25 μg/cm^3 (Table 2). The derivative was able to reduce the biofilm formation down to 30% when compared to the untreated control.

Scheme 4

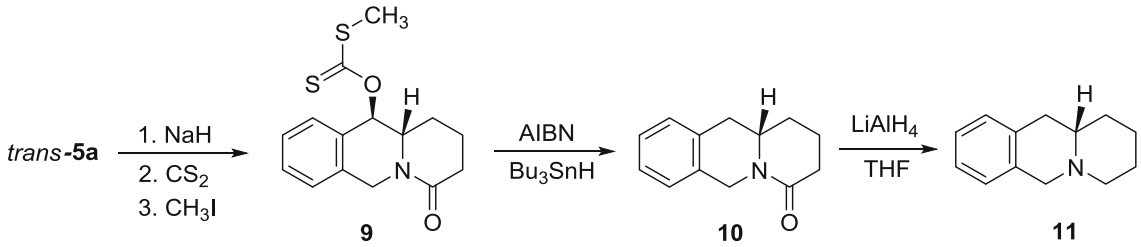

Gram-negative bacteria *E. coli* and *P. aeruginosa* were less sensitive compared to staphylococci. The growth of *E. coli* was inhibited only by the derivative **11**. The MIC_{100} value was detected at the concentration 10 μg/cm^3. *P. aeruginosa* was not inhibited by any of tested derivatives (Table 1).

Derivatives **11** and **9** with the highest antibacterial activity were tested for their potential cytotoxicity on BHK-21 and VERO cells. The IC_{50} value of the derivative **11** for BHK-21 was observed at the concentration of 40 μg/cm^3. Concerning the VERO cells, the IC_{50} value of the derivative **11** was achieved at the concentration of 50 μg/cm^3. A cytotoxic effect of derivative **9** was not observed for BHK-21 and VERO cells in the range of tested concentrations. Taking these results into account, both derivatives did not show significant toxicity on animal cell lines in the concentration range where antimicrobial activity was observed.

Concerning the mechanism of action of the QA active derivatives, some studies have reported that derivatives of QA alkaloids affect nucleic acid synthesis by inhibiting the bacterial dihydrofolate reductase (DHFR) [22]. They indicate that DHFR binds to the N-atom/NH_2 groups of its inhibitors by a strong hydrogen bond with the amino acid residues at the active site of the enzyme [23]. In accordance with our findings, the highest antibacterial activity was linked to the interaction of alkaline nitrogen in the structure (derivative **11**). It was shown that enzyme DHFR and thymidylate synthase are inhibited by phenanthroindolizidines as well as by benzoquinolizidine plant alkaloids, namely deoxytubulosin [24]. The interaction was tested on DHFR of *Lactobacillus leichmannii*. The same type of interaction was observed for *E. coli* when DHFR bound trimethoprim (TMP) frequently used in anti-infective therapy [25, 26] was also used in combination with sulfamethoxazole.

The antifungal activity was not as high as the determined antibacterial effects. The sensitivity of model fungal strains is shown in Table 3. Concerning the antifungal activity of the studied set of derivatives, *C. albicans* was more sensitive to the presence of **9** and **11** than *C. parapsilosis* (Table 3). Both yeasts were more sensitive when compared to filamentous fungi.

Model filamentous fungi were inhibited only in high concentration of derivative **11**. As described in previous results such concentration was cytotoxic for tested cell lines. Only one of the model filamentous fungi dermatophyte *T. terrestre* was inhibited by derivative **9**. The MIC_{80} value was achieved at the concentration level of 80 μg/cm^3.

Finally, potential mutagenic activity of the effective antibacterial derivative **11** was tested by the Ames test using *Salmonella typhimurium* TA98 and *S. typhimurium* TA100 without metabolic activation (Table 4).

Based on the obtained data it can be concluded that the derivative **11** did not increase the number of revertants of *S. typhimurium* TA 98 or TA 100. The number of obtained CFU of both *Salmonella* strains were comparable to observed spontaneous revertants which were significantly lower when compared to positive mutagen control 3-(5-nitro-2-furyl)acrylic acid (NFAA) (Table 4). It means that the derivative **11** does not induce point nor frameshift mutations and is therefore considered to be non-mutagenic.

Conclusion

We have achieved the asymmetric synthesis of benzoanalogues of the phenanthroquinolizidine bioactive alkaloids (−)-cryptopleurine and (−)-(15*R*)-hydroxycryptopleurine in seven or six steps, respectively, starting from available enantiopure (*S*)-2-aminoadipic acid. The latter was used as source of chirality as well as nitrogen necessary for further applications for the synthesis of these types of compounds. The highly diastereoselective reduction of the ketone function of the pure tricyclic keto-lactams **4** was achieved to provide both pure *trans*-**5a** and *cis*-**5b** alcohol-lactams in good yields. The targeted benzoquinolizidinols *trans*-**7a** and *cis*-**7a** were reached by lactam reduction in tandem with acetate deprotection. Starting from alcohol-lactam *trans*-**5a** by preparing the corresponding xanthate (*S*)-**9** followed by xanthate functionality reduction using Bu_3SnH

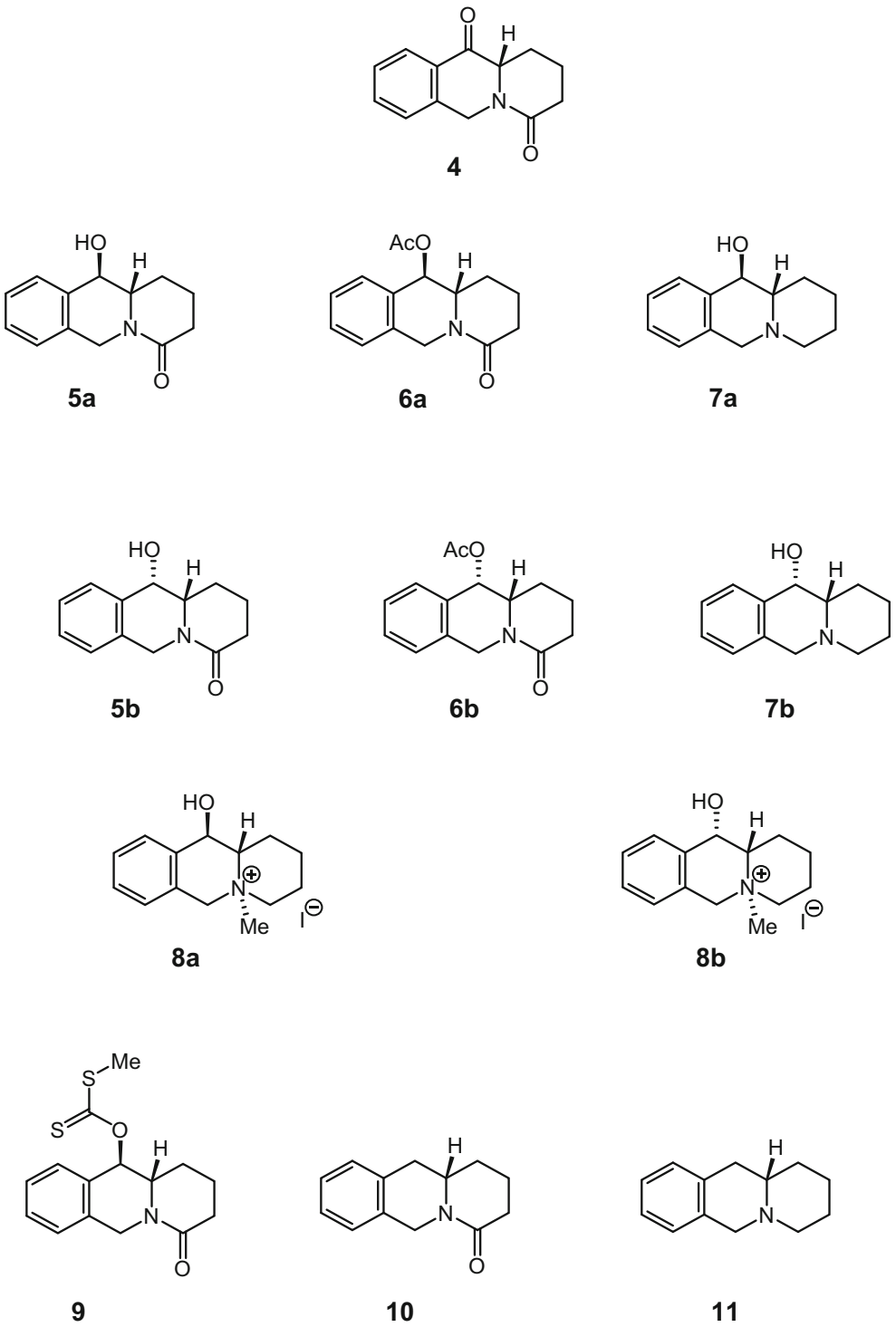

Fig. 4 Newly synthesized derivatives set assayed for antimicrobial activity

the lactam **10** was obtained. Finally, lactam **10** was directly converted to the targeted novel benzo analogue of cryptopleurine—enantiopure (*S*)-2,3,4,6,11,11a-hexahydro-1*H*-pyrido[1,2-*b*]isoquinoline (**11**) by LAH reduction. The overall yields in this linear synthesis were 32% for **7a**, 24% for **7b**, and 25% for **11**. The highest antimicrobial activity was observed in the presence of derivative **11** that significantly inhibits the growth of model bacteria especially *S. aureus*. Derivatives **9** and **11** have shown only weak antifungal activity. The most sensitive was the yeast *C. albicans*. In this work, we have shown that the derivative **11** seems to be a structure with a good antibacterial activity

Table 1 Antibacterial activity of tested compounds characterized by MIC_{100} values (μg/cm^3)

Model bacteria	Derivative	
	9 MIC_{100}	**11** MIC_{100}
S. aureus	100^s	5^s
SA21528	–	50^s
SAL18	–	50^s
S. epidermidis	100^s	10^s
E. coli	N	10^s
P. aeruginosa	N	N

N not active, *s* bacteriostatic effect, – not assayed

Table 2 Effect of derivative **11** on biofilm formation of *S. epidermidis*

Concentration derivative **11** /μg cm^{-3}	A_{570}	Biofilm intensity
0 (control)	2.6	Very strong
5	1.7	Very strong
10	0.8	Strong
25	0.7	Strong

Table 3 Antifungal activity characterized by MIC50 or MIC80 values (μg/cm^3)

Model fungi	Derivative		
		9	**11**
C. parapsilosis	MIC_{50}	50	50*
	MIC_{80}	100	–
C. albicans	MIC_{80}	50	25
A. alternata	MIC_{80}	N	N
B. cinerea	MIC_{80}	N	100
F. culmorum	MIC_{80}	N	75
T. terrestre	MIC_{80}	80	75
M. gypseum	MIC_{50}	N	100

N not active, – not detected

*The maximal inhibition was 50% with increasing concentration we did not observe increased inhibitory activity

and could be considered as a new lead structure for design of further new antimicrobial compounds by its derivatization. We suppose that its derivatization assisted by quantum chemical docking calculations with the active center of bacterial DHFR could lead to a group of new DHFR inhibitors that could be used in single as well as in synergic therapy in the future.

Table 4 Mutagenic activity of derivative **11**

Compound	Dosage /μg PD^{-1}	*Salmonella* Typhimurium	
		TA98 CFU ± SD	TA100 CFU ± SD
11	500	15 ± 1	108 ± 20
	250	13 ± 6	76 ± 13
	100	19 ± 1	95 ± 13
	50	15 ± 3	90 ± 32
	25	13 ± 6	97 ± 5
	10	14 ± 1	78 ± 14
NFAA	10	120 ± 15	1175 ± 123
SR	0	17 ± 9	90 ± 15

PD Petri dish, *SR* spontaneous revertants, *NFAA* 3-(5-nitro-2-furyl)acrylic acid—positive mutagen control

Experimental

Melting points were obtained using an STUART SMP 30 and are corrected. Commercial reagents were used without further purification. All solvents were distilled before use. Flash column liquid chromatography (FLC) was performed on silica gel Kieselgel 60 (40–63 μm, 230–400 mesh) and analytical thin-layer chromatography (TLC) was performed on aluminum plates pre-coated with either 0.2 mm (DC-Alufolien, Merck) or 0.25 mm silica gel 60 F254 (ALUGRAM-SIL G/UV254, Macherey–Nagel). The compounds were visualized by UV fluorescence and by dipping the plates in an aqueous H_2SO_4 solution of cerium sulfate/ammonium molybdate followed by charring with a heat gun. HPLC analyses were performed on Varian system 9012 with diode array Varian 9065 polychrom UV detector: column CC 250/3 Nucleosil 120-5 C18, 250 × 3 mm (Macherey–Nagel). Mobile phase: solvent A: water/acetonitrile/methanesulfonic acid (1000/25/1), solvent B: water/acetonitrile/methanesulfonic acid (25/1000/1), elution mode: gradient with 5–50% solvent B, flow rate: 0.65 cm^3/min, UV detection: 210 nm (DAD), 35 °C, 20 min. Optical rotations were measured with a POLAR L-lP polarimeter (IBZ Messtechnik) with a water-jacketed 10,000 cm cell at the wavelength of sodium line D (λ = 589 nm). Specific rotations are given in units of 10^{-1} deg cm^2 g^{-1} and concentrations are given in g/100 cm^3. Infrared spectra were recorded on a Nicolet 5700 FT-IR spectrometer as ATR discs (ATR) or as thin films on ATR plates (film). NMR spectra were recorded on a Varian VNMRS 600 MHz or INOVA 300 MHz NMR spectrometer in $CDCl_3$ or CD_3OD. Chemical shifts (δ) are quoted in ppm with the ^{1}H and ^{13}C resonance frequencies of tetramethylsilane (TMS) serving as standards for the chemical shift axis calculation. The gCOSY and NOESY

techniques were used in the assignment of ^{1}H–^{1}H relationships and the determination of relative configuration. The gHSQC and gHMBC techniques were used for the assignment of the ^{1}H–^{13}C relationships. Only apparent splitting constants are written in the compound characterization data instead of coupling constants because of the difficulty of extraction of the latter from complex multiplet patterns. Elemental high-resolution spectrometry was performed on Micromass Q-Tof Micro MS system with ESI^{+} ionization (measured mass represents $M + H^{+}$).

The synthesis of (*S*)-1,2,3,11a-tetrahydro-4*H*-pyrido[1,2-*b*]isoquinoline-4,11(6*H*)-dione (**4**) and (11*R*,11a*S*)-11-hydroxy-1,2,3,6,11,11a-hexahydro-4*H*-pyrido[1,2-*b*]-isoquinolin-4-one (**5a**) is described in [16].

(11*S*,11a*S*)-11-Hydroxy-1,2,3,6,11,11a-hexahydro-4*H*-pyrido[1,2-*b*]isoquinolin-4-one (5b, $C_{13}H_{15}NO_2$) The freshly crystallized keto-lactam **4** (1.29 g, 6 mmol) was dissolved in 120 cm^3 dry THF and cooled to − 45 °C with stirring. 1 M solution of L-Selectride in THF (18 cm^3, 18 mmol) was added (30 min) dropwise via a syringe and the reaction mixture was stirred for 2.5 h at − 40 °C, then it was gradually quenched with 5 cm^3 methanol, 5 cm^3 H_2O, 7.5 cm^3 sodium hydroxide aqueous solution (1 M), and 7.5 cm^3 hydrogen peroxide (30% in water) at − 5 °C. The reaction mixture was then stirred 1 h at + 5 °C, concentrated under vacuum (40 °C water bath and 1 mbar pressure) and extracted with CH_2Cl_2 (3 × 50 cm^3). The combined organic layers were washed with water and brine (2 × 20 cm^3) and dried over anhydrous $MgSO_4$. After filtration, the filtrate was concentrated in vacuo to afford a solid as a mixture of *cis* and *trans* diastereomers **5b** and **5a** (1.1 g, 83%) in 95:5 ratio (from ^{1}H NMR spectra). Recrystallization of the solid from AcOEt gave **5b** (780 mg, 60%) as colorless crystals. M.p.: 178.9–182.3 °C; $[\alpha]_D^{23}$ = + 11.12 (*c* = 1.01, MeOH); R_f = 0.2 (CH_2Cl_2/acetone, 8:1); IR (ATR): $\bar{\nu}$ = 3334, 1614, 1582, 1481, 1444, 1364, 1344, 1333, 1242, 1190, 1172, 1118, 1108, 1077, 1037, 1008, 982, 952, 896, 797, 749, 721, 663, 625, 564, 514, 513, 481, 470, 439 cm^{-1}; ^{1}H NMR (300 MHz, CD_3OD): δ = 7.35–7.19 (m, 4H), 5.18 (d, *J* = 17.8 Hz, 1H), 4.50 (d, *J* = 1.6 Hz, 1H), 4.30 (d, *J* = 17.8 Hz, 1H), 3.72–3.64 (m, 1H), 2.47–2.37 (m, 2H), 2.24–2.00 (m, 3H), 1.84–1.66 (m, 1H) ppm; ^{13}C NMR (75 MHz, CD_3OD): δ = 173.7 (s), 137.6 (s), 133.8 (s), 130.2 (d), 129.7 (d), 127.9 (d), 127.6 (s), 71.1 (d), 58.9 (d), 45.8 (t), 33.4 (t), 26.5 (t), 20.1 (t) ppm; HRMS: *m/z* calcd for $C_{13}H_{15}NO_2$ $[M + H]^{+}$: 218.1176, found 218.1165.

(11*R*,11a*S*)-4-Oxo-1,3,4,6,11,11a-hexahydro-2*H*-pyrido[1,2-*b*]isoquinolin-11-yl acetate (6a, $C_{15}H_{17}NO_3$) To a solution of 1.63 g freshly crystallized *trans*-**5a** (7.5 mmol) in 45 cm^3 dry CH_2Cl_2 was added 1.53 g acetic anhydride (1.41 cm^3, 22.5 mmol), 92 mg 4-(dimethylamino)pyridine (DMAP, 0.75 mmol), and 1.53 g triethylamine (2.12 cm^3). The reaction mixture was stirred until the disappearance of the starting material (monitored by TLC). The mixture was diluted with 50 cm^3 CH_2Cl_2 and quenched with a saturated aqueous $NaHCO_3$ solution. The aqueous layer was extracted with 50 cm^3 CH_2Cl_2 and the organic layers were washed with a saturated aqueous $CuSO_4$ solution, 25 cm^3 HCl (10%), 30 cm^3 Na_2CO_3 (25%), and water, dried over $MgSO_4$, and concentrated under vacuum. An oily matter, which quickly crystallized on standing, was obtained in the yield of 1.67 g, 86%. Recrystallization from a mixture of AcOEt/*i*-hexane gave 1.36 g (70%) of **6a** as colorless crystals. R_f = 0.72 (CH_2Cl_2/acetone, 4:1); m.p.: 99.2–102.4 °C; $[\alpha]_D^{23}$ = + 22.16 (*c* = 1.02, THF); IR (ATR): $\bar{\nu}$ = 1723, 1641, 1463, 1445, 1417, 1370, 1360, 1330, 1237, 1187, 1174, 1030, 1016, 980, 902, 795, 759, 680, 654, 628, 544, 528, 511, 466, 438 cm^{-1}; ^{1}H NMR (300 MHz, $CDCl_3$): δ = 7.32–7.10 (m, 4H), 6.08 (d, *J* = 9.7, 1H), 5.50 (d, *J* = 17.2 Hz, 1H), 4.15 (d, *J* = 17.2 Hz, 1H), 3.67 (dt, *J* = 9.7, 4.9 Hz, 1H), 2.51–2.37 (m, 2H), 2.23 (s, 3H), 2.10–1.91 (m, 2H), 1.90–1.73 (m, 2H) ppm; ^{13}C NMR (75 MHz, $CDCl_3$): δ = 171.1 (s), 169.7 (s), 133.6 (s), 133.5 (s), 128.3 (d), 127.11 (d), 126.5 (d), 126.4 (d), 70.4 (d), 57.0 (d), 44.7 (t), 32.6 (t), 24.7 (t), 21.3 (q), 17.8 (t) ppm; HRMS: *m/z* calcd for $C_{15}H_{17}NO_3$ $[M + H]^{+}$: 260.1281, found 260.1272.

(11*S*,11a*S*)-4-Oxo-1,3,4,6,11,11a-hexahydro-2*H*-pyrido-[1,2-*b*]isoquinolin-11-yl acetate (6b, $C_{15}H_{17}NO_3$) This product was obtained from 1.52 g freshly crystallized *cis*-**5b** (7.0 mmol), 45 cm^3 CH_2Cl_2, 1.43 g acetic anhydride (1.31 cm^3, 14 mmol), 85 mg 4-(dimethylamino)pyridine (DMAP, 0.7 mmol), and 1.42 g triethylamine (1.95 cm^3) in the same way as for **6a**. Yield 1.34 g (74.1%); colorless crystals; R_f = 0.67 (CH_2Cl_2/acetone, 4:1); m.p.: 144.3–152.4 °C; $[\alpha]_D$ = + 28.11 (*c* = 1.02, THF); IR (ATR): $\bar{\nu}$ = 2952, 1735, 1637, 1591, 1443, 1417, 1369, 1224, 1190, 1163, 1043, 1032, 1019, 976, 945, 898, 764, 743, 548, 518, 463 cm^{-1}; ^{1}H NMR (300 MHz, CD_3OD): δ = 7.43–7.31 (m, 2H), 7.28–7.22 (m, 2H), 5.92 (d, *J* = 1.7 Hz, 1H), 5.12 (d, *J* = 17.9 Hz, 1H), 4.40 (d, *J* = 17.9 Hz, 1H), 3.94-3.86 (m, 1H), 2.51–2.40 (m, 2H), 2.20–1.94 (m, 2H), 1.92–1.70 (m, 2H) ppm; ^{13}C NMR (75 MHz, CD_3OD): δ = 173.4 (s), 172.1 (s), 134.6 (s), 133.8 (s), 1230.7 (d), 130.6 (d), 128.0 (d), 1267.8 (d), 72.3 (d), 57.5 (d), 45.8 (t), 33.3 (t), 26.6 (t), 21.0 (q), 20.0(t) ppm; HRMS: *m/z* calcd for $C_{15}H_{17}NO_3$ (259.31) $[M + H]^{+}$: 260.1281, found 260.1276.

(11*R*,11a*S*)-1,3,4,6,11,11a-Hexahydro-2*H*-pyrido[1,2-*b*]isoquinolin-11-ol (7a, $C_{13}H_{17}NO$) Lithium aluminum hydride (584 mg, 15.4 mmol) was added to a solution of 800 mg freshly crystallized acetyl derivative **6a** (3.1 mmol) in 25 cm^3 dry THF at room temperature and the mixture was then heated under reflux for 1.5 h. The slurry was then

warmed to ambient temperature and after additional 40 min was carefully quenched with 2:1 (w/w) $Na_2SO_4.10H_2O$:Celite (15 g, gas evolution!). Dry diethyl ether (20 cm^3) was then added and after 30 min. The white suspension was filtered, dried over $MgSO_4$, and concentrated in vacuo to give a light yellow solid (548 mg, 90%). Recrystallization of the solid from *n*-hexane gave pure alcohol **7a** as pale cream-colored crystals (433 mg, 68.7%). M.p.: 137.2–139.1 °C; $[\alpha]_D^{23} = +64.51$ (c = 1.01, MeOH); R_f = 0.39 (CH_2Cl_2/acetone, 1:1); IR (ATR): $\bar{\nu}$ = 3332, 2929, 1490, 1453, 1431, 1349, 1270, 1124, 1047, 1028, 877, 796, 743, 714, 637, 552, 461, 450 cm^{-1}; ^{1}H NMR (300 MHz, $CDCl_3$): δ = 7.47–7.42 (m, 1H), 7.21 (dt, J = 1.6, 7.3 Hz, 1H), 7.17 (dt, J = 1.6, 7.3 Hz, 1H), 7.01-6.95 (m, 1H), 4.30 (d, J = 8.4 Hz, 1H), 3.74 (d, J = 15.2 Hz, 1H), 3.32 (d, J = 15.2 Hz, 1H), 2.99 (dtd, J = 11.4, 3.3, 1.7 Hz, 1H), 2.29–2.20 (m, 1H), 2.11 (dt, J = 11.3, 4.2 Hz, 1H), 1.95 (dt, J = 3.4, 8.7 Hz, 1H), 1.86–1.77 (m, 1H), 1.72–1.54 (m, 2H), 1.38–1.16 (m, 2H) ppm; ^{13}C NMR (75 MHz, $CDCl_3$): δ = 137.3 (s), 134.1 (s), 127.4 (d), 127.0 (d), 126.9 (d), 125.6 (d), 73.2 (d), 65.9 (d), 58.1 (t), 56.2 (t), 30.4 (t), 25.4 (t), 24.0 (t) ppm; HRMS: *m/z* calcd for $C_{13}H_{17}NO$ (203.29) $[M + H]^+$: 204.1383, found 204.1369.

(11*S*,11a*S*)-1,3,4,6,11,11a-Hexahydro-2*H*-pyrido[1,2-*b*]isoquinolin-11-ol (7b, $C_{13}H_{17}NO$) This product was obtained from 800 mg freshly crystallized acetyl derivative **6b** (3.1 mmol) and 584 mg lithium aluminum hydride (15.4 mmol) in 30 cm^3 dry THF in the same way as for **7a**. Yield 463 mg (73.5%), colorless crystals. M.p.: 137.2–139.1 °C (*i*-hexane); R_f = 0.17 (CH_2Cl_2/acetone, 1:1); $[\alpha]_D^{22} = +52.66$ (c = 1.01, MeOH); IR (ATR): $\bar{\nu}$ = 3176, 2923, 2761, 1490, 1455, 1435, 1413, 1350, 1289, 1274, 1109, 1088, 1067, 1041, 988, 941, 921, 879, 839, 801, 752, 730, 702, 627, 584, 445 cm^{-1}; ^{1}H NMR (600 MHz, CD_3OD): δ = 7.36–7.32 (m, 1H), 7.25–7.20 (m, 2H), 7.10–7.05 (m, 1H), 4.33 (d, J = 2.8 Hz, 1H), 3.85 (d, J = 15.5 Hz, 1H), 3.30 (d, J = 15.5 Hz, 1H), 3.13–3.07 (m, 1H), 2.30 (td, J = 11.3, 2.9 Hz, 1H), 2.16 (dt, J = 3.0, 12.0 Hz, 1H), 2.00–1.91 (m, 1H), 1.73–1.67 (m, 2H), 11.65–1.57 (m, 1H), 1.63 (tq, J = 3.7, 12.8 Hz, 1H), 1.42 (qt, J = 3.8, 13.0 Hz, 1H) ppm; ^{13}C NMR (151 MHz, CD_3OD): δ = 137.6 (s), 135.1 (s), 130.9 (d), 128.9 (d), 127.8 (d), 126.9 (d), 70.2 (d), 64.4 (d), 59.2 (t), 57.4 (t), 28.5 (t), 26.5 (t), 25.3 (t) ppm; HRMS: *m/z* calcd for $C_{13}H_{17}NO$ (203.29) $[M + H]^+$: 204.1383, found 204.1371.

(5*S*,11*R*,11a*S*)-11-Hydroxy-5-methyl-1,2,3,4,5,6,11,11a-octahydropyrido[1,2-*b*]isoquinolinium iodide (8a, $C_{14}H_{20}INO$) Methyl iodide (213 mg, 0.095 cm^3, 1.5 mmol) was added to a solution of 203 mg **7a** (1 mmol) in 5 cm^3 dry acetone and the mixture was allowed to stand at room temperature for 12 h. The colorless crystals were filtered off and washed with 2 cm^3 dry acetone to provide pure isoquinolinium iodide **8** (280 mg, 81%). M.p.: 237.4–239.6 °C (methanol/diethyl ether); $[\alpha]_D^{22} = +24.97$ (c = 1.02, MeOH); IR (ATR): $\bar{\nu}$ = 3228, 1495, 1469, 1451, 1435, 1415, 1357, 1268, 1168, 1090, 1039, 1003, 979, 957, 929, 918, 873, 793, 749, 638, 549, 523, 495 cm^{-1}; ^{1}H NMR (600 MHz, D_2O): δ = 7.64 (d, J = 7.8 Hz, 1H), 7.54 (t, J = 7.6 Hz, 1H), 7.47 (t, J = 7.6 Hz, 1H), 7.27 (d, J = 7.7 Hz, 1H), 4.79 (d, J = 15.2 Hz, 1H), 4.75 (d, J = 9.8 Hz, 1H), 4.55 (d, J = 15.2 Hz, 1H), 3.72–3.67 (m, 1H), 3.61–3.54 (m, 2H), 3.03 (s, 3H), 2.48–2.40 (m, 1H), 2.00–1.92 (m, 1H), 1.90–1.80 (m, 2H), 1.69 (tq, J = 4.2, 13.4 Hz, 1H) ppm; ^{13}C NMR (151 MHz, D_2O): δ = 135.9 (s), 132.1 (d), 131.9 (d), 130.7 (d), 129.3 (d), 128.8 (s), 73.1 (d), 69.8 (d), 69.0 (t), 68.8 (t), 42.7 (q), 25.9 (t), 24.1 (t), 22.3 (t) ppm.

(5*S*,11*S*,11a*S*)-11-Hydroxy-5-methyl-1,2,3,4,5,6,11,11a-octahydropyrido[1,2-*b*]isoquinolin-5-ium iodide (8b, $C_{14}H_{20}INO$) This product was obtained from 203 mg freshly crystallized *cis*-**7b** (1 mmol), 213 mg methyl iodide (0.095 cm^3, 1.5 mmol), and 5 cm^3 dry acetone in the same way as for **8a**. Yield 270 mg (78%); colorless crystals; m.p.: 237.4–239.6 °C (methanol/diethyl ether); $[\alpha]_D^{21} = +10.75$ (c = 1.01, MeOH); IR (ATR): $\bar{\nu}$ = 3311, 2938, 1495, 1445, 1303, 1277, 1174, 1094, 1017, 970, 935, 911, 865, 797, 747, 667, 624, 580, 504, 451 cm^{-1}; ^{1}H NMR (600 MHz, CD_3OD): δ = 7.55 (dd, J = 1.3, 7.7 Hz, 1H), 7.47 (tt, J = 1.1, 7.7 Hz, 1H), 7.42 (td, J = 1.4, 7.5 Hz, 1H), 7.25 (d, J = 7.7 Hz, 1H), 4.82 (d, J = 1.7 Hz, 1H), 4.70 (d, J = 15.2 Hz, 1H), 4.62 (d, J = 15.2 Hz, 1H), 3.90 (td, J = 3.4, 12.4 Hz, 1H), 3.73–3.68 (m, 1H), 3.59 (dt, J = 3.2, 13.4 Hz, 1H), 3.13 (s, 3H), 2.38–2.29 (m, 1H), 2.20–2.11 (m, 1H), 2.10-2.03 (m, 1H), 1.98–1.90 (m, 2H), 1.80 (tq, J = 13.4, 4.2 Hz, 1H) ppm; ^{13}C NMR (151 MHz, CD_3OD): δ = 135.9 (s), 131.3 (d), 130.4 (d), 130.2 (d), 127.7 (d), 127.0 (s), 71.3 (d), 67.7 (t), 67.6 (t), 66.9 (d), 43.1 (q), 23.9 (t), 23.3 (t), 21.4 (t) ppm.

***S*-Methyl *O*-[(11*R*,11a*S*)-4-oxo-1,3,4,6,11,11a-hexahydro-2*H*-pyrido[1,2-*b*]isoquinolin-11-yl]carbonodithioate (9, $C_{15}H_{17}NO_2S_2$)** A mixture of 1.31 g freshly crystallized alcohol *trans*-**5a** (6 mmol), 228 mg NaH (60% in oil, 12 mmol) and 25 mg imidazole in 55 cm^3 dry THF was refluxed with stirring for 30 min under nitrogen. CS_2 (3.6 cm^3, 60 mmol) in 2 cm^3 THF was then added to the reaction mixture. After refluxing for further 45 min, 4.4 cm^3 MeI (70 mmol) was added and the reflux continued for another 30 min. The reaction mixture was brought to room temperature and quenched with iced water containing acetic acid (0.3 cm^3), diluted with water and extracted with CH_2Cl_2 (3 × 50 cm^3). The combined organic layer was washed with 15% Na_2CO_3 solution and brine and dried. The solvent was removed in vacuo, and the residue was

chromatographed (100 g, 35 × 750 mm, CH_2Cl_2 as eluent) on silica gel to give the thiocarbamate as pale pink solid (1.65 g, 89%) which after recrystallization from *n*-heptane gave **9** as a colorless crystals (1.50 g, 81%). M.p.: 171.2–171.6 °C; $[\alpha]_D^{22} = -28.8$ (c = 1.05, MeOH); R_f = 0.56 (CH_2Cl_2/*i*-PrOH; 10:1); IR (ATR): $\bar{\nu}$ = 3261, 3057, 2945, 2920, 1650, 1498, 1461, 1437, 1419, 1359, 1331, 1244, 1198, 1168, 1099, 1049, 1019, 992, 955, 941, 908, 894, 877, 849, 814, 748, 728, 667, 630, 586, 534, 464, 439, 407 cm^{-1}; ^1H NMR (600 MHz, $CDCl_3$): δ = 7.29 (td, J = 7.4, 1.5 Hz, 1H), 7.24 (t, J = 7.5 Hz, 1H), 7.20 (d, J = 7.6 Hz, 1H), 7.19 (d, J = 7.6 Hz, 1H), 7.08 (d, J = 9.8 Hz, 1H), 5.55 (d, J = 17.2 Hz, 1H), 4.16 (d, J = 17.2 Hz, 1H), 3.86 (dt, J = 9.5, 4.5 Hz, 1H), 2.66 (s, 3H), 2.57–2.37 (m, 2H), 2.06–1.96 (m, 2H), 1.95–1.89 (m, 1H), 1.84–1.75 (m, 1H) ppm; ^{13}C NMR (151 MHz, $CDCl_3$): δ = 217.4 (s), 169.5 (s), 133.3 (s), 132.6 (s), 128.4 (d), 126.9 (d), 126.4 (d), 126.2 (d), 78.3 (d), 56.7 (d), 44.4 (t), 32.3 (t), 24.0 (t), 19.5 (q), 17.8 (t) ppm; HRMS: *m/z* calcd for $C_{15}H_{17}NO_2S_2$ (307.43) $[M + H]^+$: 308.0701 found 308.0691.

(*S*)-1,2,3,6,11,11a-Hexahydro-4*H*-pyrido[1,2-*b*]isoquinolin-4-one (10, $C_{13}H_{15}NO$) To a boiling solution of 1.5 g thiocarbamate **9** (4.88 mmol) in 50 cm^3 toluene containing 2 cm^3 AIBN (0.2 M solution in toluene) was added 2 cm^3 tributyltin hydride (7.31 mmol) in an argon atmosphere, and the reaction mixture was refluxed for 1 h. The reaction mixture was brought to room temperature, the solvent removed, and the crude product chromatographed on silica gel (80 g, 35 × 750 mm). Elution with CH_2Cl_2/cyclohexane (1:3) removed the organotin impurities. Further elution with CH_2Cl_2/MeOH (80:1) furnished the amide (864 mg, 88%) as colorless oil, which quickly crystallized on standing. Recrystallization from *i*-hexane provided **10** as colorless crystals (737 mg, 75%). M.p.: 78.9–79.7 °C; $[\alpha]_D^{22} = +75.2$ (c = 1.06, MeOH); R_f = 0.50 (CH_2Cl_2/*i*-PrOH; 10:1); IR (ATR): $\bar{\nu}$ = 3246, 3030, 2945, 2839, 1628, 1582, 1463, 1440, 1415, 1361, 1349, 1332, 1246, 1183, 1171, 1160, 1104, 1039, 991, 926, 891, 849, 749, 710, 673, 633, 606, 524, 515, 448, 435 cm^{-1}; ^1H NMR (600 MHz, $CDCl_3$): δ = 7.21–7.12 (m, 3H), 7.09 (dd, J = 7.1, 1.9 Hz, 1H), 5.26 (d, J = 17.5 Hz, 1H), 4.29 (d, J = 17.5 Hz, 1H), 3.66–3.59 (m, 1H), 2.88 (dd, J = 15.8, 11.1 Hz, 1H), 2.78 (dd, J = 15.7, 3.7 Hz, 1H), 2.52–2.42 (m, 2H), 2.17–2.09 (m, 1H), 2.00–1.85 (m, 1H), 1.82–1.75 (m, 1H), 1.75-1.67 (m, 1H) ppm; ^{13}C NMR (151 MHz, $CDCl_3$): δ = 169.8 (s), 133.9 (s), 133.0 (d), 128.3 (d), 126.8 (d), 126.7 (d), 126.6 (d), 53.7 (d), 45.1 (t), 37.0 (t), 32.9 (t), 29.5 (t), 18.9 (t) ppm; HRMS: *m/z* calcd for $C_{13}H_{15}NO$ (201.27) $[M + H]^+$: 202.1226 found 202.1219.

(*S*)-1,3,4,6,11,11a-Hexahydro-2*H*-pyrido[1,2-*b*]isoquinoline (11) Lithium aluminum hydride (750 mg, 20 mmol) was added to a solution of 550 mg lactam **10** (2.73 mmol) in 30 cm^3 dry THF at room temperature and the mixture was then heated under reflux for 2 h. The resulting mixture was cooled, NH_4Cl and water were added cautiously until the lithium complex was decomposed. The mixture was then diluted with 10 cm^3 water and 50 cm^3 dichloromethane. The CH_2Cl_2 layer was separated and the aqueous layer extracted with CH_2Cl_2 (2 × 20 cm^3). The combined extracts were washed with water, brine, dried over $MgSO_4$, and concentrated in vacuo to give a pale yellow, low-melting solid (449 mg, 87.7%). Distillation on Kugelrohr (135 °C/10.8 Pa) gave pure amine **11** as colorless crystals (404 mg, 78.9%); m.p.: 44.1–45.2 °C. Analytically pure material was obtained by recrystallization from dry *n*-hexane. M.p.: 44.8–45.3 °C; $[\alpha]_D^{20} = +42.26$ (c = 0.5, CH_2Cl_2); R_f = 0.53 (AcOEt—petroleum ether—Et_3N, 8:2:1); [27] $[\alpha]_D^{20} = +26.0$ (c = 0.5, CH_2Cl_2); R_f = 0.25 ($CHCl_3$—MeOH, 10:1), yellow oil; or [28] $[\alpha]_D^{20} = +29.3$ (c = 0.28); m.p.: 42.0–47.0 °C; IR (ATR): $\bar{\nu}$ = 3062, 3026, 2933, 2850, 2750, 2675, 1493, 1454, 1439, 1348, 1296, 1250, 1174, 1116, 1063, 937, 874, 734, 638, 575, 542, 430 cm^{-1}; ^1H NMR (600 MHz, $CDCl_3$): δ = 7.12–7.06 (m, 2H), 7.04 (d, J = 7.1 Hz, 1H), 7.00 (d, J = 7.2 Hz, 1H), 3.85 (d, J = 15.1 Hz, 1H), 3.38 (d, J = 15.1 Hz, 1H), 3.07 (d, J = 11.3 Hz, 1H), 2.77 (dd, J = 16.5, 3.4 Hz, 1H), 2.70 (dd, J = 10.5, 16.5 Hz, 1H), 2.27–2.18 (m, 1H), 2.11 (td, J = 3.0, 11.3 Hz, 1H), 1.88–1.75 (m, 2H), 1.74–1.62 (m, 2H), 1.40–1.28 (m, 2H) ppm; ^{13}C NMR (151 MHz, $CDCl_3$): δ = 134.3 (s), 133.9 (s), 127.9 (d), 126.1 (d), 125.9 (d), 125.5 (d), 58.4 (t), 58.2 (d), 56.1 (t), 36.8 (t), 33.7 (t), 25.9 (t), 24.3 (t) ppm; HRMS: *m/z* calcd for $C_{13}H_{17}N$ (187.29) $[M + H]^+$: 188.1434 found 188.1428.

X-ray diffraction

The X-ray diffraction data for the crystals **8a** and **9** were collected at 298 K on a four-circle diffractometer Xcalibur, Ruby, Gemini using graphite-monochromated radiation. The structures were solved by direct (heavy) methods and refined by full-matrix least-squares using the SHELXL [29], ShelXle [30], and OLEX [31] programs. All the non-hydrogen atoms in the molecules were refined with anisotropic atomic displacement parameters. All figures were made using the program DIAMOND [32].

Crystallographic data for the structures in this paper have been deposited with the Cambridge Crystallographic Data Centre as supplementary publication nos. CCDC

1815854 for **8a** and 1815853 for **9**. Copies of the data can be obtained, free of charge, on application to CCDC, 12 Union Road, Cambridge CB2 1EZ, UK, fax: + 44-(0)1223-336033 or e-mail: deposit@ccdc.cam.ac.uk.

Antimicrobial activity in vitro of newly synthesized derivatives

Antimicrobial activity of newly synthesized derivatives was assayed on *Staphylococcus epidermidis* CCM 7221, *Staphylococcus aureus* CCM 3953, two *S. aureus* isolates described as methicillin resistant (MRSA) SA21528 and SAL18 (hospital isolates), and on *γ-Proteobacteria Escherichia coli* CCM 3988, *Pseudomonas aeruginosa* CCM 1959 (Czech Collection of Microorganisms, Masaryk University, Brno, Czech Republic). Antibacterial and antifungal activities on model yeast *Candida albicans* SC 5314 and *Candida parapsilosis* ATCC 22019 were evaluated by the micro-dilution method [33, 34]. The sensitivity of filamentous fungi *Fusarium culmorum* CCM F-21, *Botrytis cinerea* CCM F-16 (Czech Collection of Microorganisms, Masaryk University, Brno, Czech Republic), *Alternaria alternata* (Collection of Microorganisms of Department of Biochemistry and Microbiology, Faculty of Chemical and Food Technology STU, Bratislava, Slovakia) *Microsporum gypseum* and *Trichophyton terrestre* (Laboratory of Medical Mycology, Postgraduate Medical Institute, Bratislava, Slovakia) was studied by the macrodilution method [35]. Subcultures of microorganisms were prepared separately in Petri dishes containing appropriate agarized growth medium and incubated at 37 °C for 24 h (bacteria); 48 h (model yeasts) and at 25 °C for 96 h for filamentous fungi except *M. gypseum* and *T. terrestre*—their cultivation time was prolonged for 2 weeks according to their growth rate. The assessment of antibacterial and antifungal activities was expressed as the concentration of the derivative inhibiting the growth of bacteria by 50% (MIC_{50}), 80% MIC_{80} resp. 100% MIC_{100} values. The $MIC_{50,}$ MIC_{80} and MIC_{100} values were derived from the dosage response curves. Chromatographically pure compounds were dissolved in dimethyl sulfoxide (DMSO) Sigma-Aldrich Ltd; (Steinheim, Germany); its final concentration never exceeded 1.0 vol% either in control or in treated samples.

Bacterial biofilm formation in vitro

Biofilm formation was assayed after crystal violet staining in 96-well polystyrene microtiter plates for 24 h. Briefly, *S. epidermidis* CCM 7221 was cultivated for 16 h in Mueller–Hinton growth medium (MHB) (Biolife, Milano, Italy) under shaking (200 rpm). Cultures were diluted to a cell density of $10^7/cm^3$ into MHB. 198 mm^3 aliquots of fresh diluted cells were added into wells of the 96 flat bottom well polystyrene microplate (Sarstedt, Nümbrecht, Germany). For biofilm inhibition assay 2 mm^3 of appropriate concentrated (100 times) derivative **11** solution (diluted in DMSO) was added to each well of the plate. As controls, 10 wells of each microtiter plate were handled in an identical fashion, except that no derivative solution was added to the cells. Cells were cultivated without shaking at 37 °C for the biofilm formation. After that, plates were incubated without shaking at 37 °C for 24 or 48 h. Formed biofilm was evaluated by the crystal violet staining [36]. Biofilm intensity was evaluated according to the observed absorbance values as weak, medium or strong (A570 < 0.1–0.29 > weak biofilm formation; A570 < 0.3–0.5 > medium biofilm formation; A570 < 0.5–0.99 > strong biofilm formation; A570 > 1.0). All experiments were performed in six parallel measurements.

Ames test for evaluation on potential mutagenicity

Assessment of potential mutagenicity was performed using classical plate incorporation method [37] without metabolic activation using *Salmonella* Typhimurium TA 98 and TA100. As positive mutagen 3-(5-nitro-2-furyl)acrylic acid (NFAA) was used. Positive response was defined as a reproducible twofold increase of revertants with dose response relationship.

The cytotoxicity assay on BHK-21 and VERO cell lines

The cytotoxicity of the derivatives **9** and **11** was tested on BHK-21 (BHK-21 stabilized adherent cell line derived in 1962 from the kidney of day-old hamster, fibroblast cells) and VERO (VERO-stabilized adherent cell line derived from kidney of Cercopithecus aethiops, fibroblast cells) cell lines in 96-well microplates plates at the density of 1.8×10^4 cells/well in 100 mm^3 of DMEM growth media supplemented with 10% FBS, 1% penicillin/streptomycin, 1% L-glutamine and 0.1% gentamicin. Cells were treated with 1 mm^3 of derivative **9** or **11** dissolved in DMSO (in concentration range 1-100 $\mu g/cm^3$) at 37 °C for 24 h in 5% CO_2 atmosphere. After 24 h of incubation at 37 °C, 100 mm^3 of MTT (3-[4,5-dimethylazol-2-yl]-2,5-diphenyltetrazolium bromide) 5 mg/cm^3 in PBS was added. The cells were further incubated for 4 h and the reaction was stopped with 200 mm^3 DMSO that was added to each well. Subsequently, absorbance values at the wavelength of 570 nm were measured and cell viability was compared to untreated

controls—cells incubated with 1% DMSO (derivativés solvent). Finally, cells' survival rate (%) was calculated according the formula

$$\%\ \text{Survival rate} = \left(A_{570\text{sample}} - A_{570\text{blank}}\right) / \left(A_{570\text{control}} - A_{570\text{blank}}\right) \times 100\,\%,$$

and IC_{50} values were evaluated based on the cell survival curve.

Acknowledgements This work was supported by the Grant Agency of the Slovak Republic (Grant no. 1/0371/16). This contribution is also the result of the project: Research Center for Industrial Synthesis of Drugs, ITMS 26240220061, supported by the Research & Development Operational Programme funded by the ERDF.

References

1. Laxminarayan R, Duse A, Wattal C, Zaidi AK, Wertheim HF, Sumpradit N, Vlieghe E, Hara GL, Gould IM, Goossens H, Greko C, So AD, Bigdeli M, Tomson G, Woodhouse W, Ombaka E, Peralta AQ, Qamar FN, Mir F, Kariuki S, Bhutta ZA, Coates A, Bergstrom R, Wright GD, Brown ED, Cars O (2013) Lancet Infect Dis 13:1057
2. Gundersen LL, Charnock C, Negussie AH, Rise F, Teklu S (2007) Eur J Pharm Sci 30:26
3. Cushnie TT, Cushnie B, Lamb AJ (2014) Int J Antimicrob Agents 44:377
4. Bunsupa S, Yamazaki M, Saito K (2012) Front Plant Sci 3:239
5. Kubo H, Kobayashi J, Higashiyama K, Kamei J, Fujii Y, Ohmiya S (2000) Biol Pharm Bull 23:1114
6. Guarna A, Occhiato EG, Machetti F, Trabocchi A, Scarpi D, Danza G, Comerci A, Serio M (2001) Bioorg Med Chem 9:1385
7. Vrábel V, Sivy J, Šafař P, Marchalín Š (2016) Acta Chim Slov 9:180
8. Facchini PJ (2001) Annu Rev Plant Physiol Plant Mol Biol 52:29
9. Han R, Takahashi H, Nakamura M, Bunsupa S, Yoshimoto N, Yamamoto H, Saito K (2015) Bull Biol Pharm 38:87
10. Huang W, Kim SJ, Liu J, Zhang W (2015) Org Lett 17:5344
11. Santhosh RS, Suriyanarayanan B (2014) Planta Med 80:9
12. Wahba AE, Peng J, Kudrimoti S, Tekwani BL, Hamann MT (2009) Bioorg Med Chem 17:7775
13. Locher HH, Ritz D, Pfaff P, Gaertner M, Knezevic A, Sabato D, Schroeder S, Barbaras D, Gademann K (2010) Chemotherapy 56:318
14. Kumar NS, Dullaghan EM, Finlay BB, Gong H, Reiner NE, Selvam JJP, Zoraghi R (2014) Bioorg Med Chem 22:1708
15. Sivý J, Vrábel V, Marchalín Š, Šafář P (2015) Asian J Chem 27:2635
16. Šafář P, Marchalín Š, Šoral M, Moncol J, Daïch A (2017) Org Lett 19:4742
17. Marchalín Š, Szemes F, Bar N, Decroix B (1999) Heterocycles 50:445
18. Šafář P, Žúžiová J, Bobošikova M, Marchalín Š, Prónayová N, Comesse S (2009) Tetrahedron Asymmetry 20:2137
19. Šafář P, Žúžiová J, Marchalín Š, Tóthova E, Prónayová N, Švorc Ľ, Vrábel V, Daïch A (2009) Tetrahedron Asymmetry 20:626
20. Šafář P, Marchalín Š, Prónayová N, Vrábel V, Lawson AM, Othman M, Daich A (2016) Tetrahedron 72:3221
21. Rasmussen MO, Delair P, Greene AE (2001) J Org Chem 66:5438
22. Rao KN, Venkatachalam SR (2000) Toxicol In Vitro 14:53
23. Rao KN (1998) Indian J Biochem Biophys 35:229
24. Zakrzewski SF (1963) J Biol Chem 238:1485
25. Baker DJ, Beddell CR, Champness JN, Goodford PJ, Norrington FEA, Smith DR, Stammers DK (1981) FEBS Lett 126:49
26. Markowitz N, Quinn EL, Saravolatz LD (1992) Ann Intern Med 117:390
27. García D, Foubelo F, Yus M (2010) Eur J Org Chem 2010:2893
28. Yamada S, Kunieda T (1967) Chem Pharm Bull 15:490
29. Sheldrick GM (2015) Acta Cryst A71:3
30. Hübschle CB, Sheldrick GM, Dittrich B (2011) Appl Cryst 44:1281
31. Dolomanov OV, Bourhis LJ, Gildea RJ, Howard JAK, Puschmann HJ (2009) Appl Cryst 42:339
32. Brandenburg K (1999) DIAMOND. Crystal Impact GbR, Bonn
33. Clinical and Laboratory Standards Institute (CLSI) (1996) Reference method for broth dilution antifungal susceptibility testing yeast; approved standard. USA
34. Clinical and Laboratory Standards Institute (CLSI) (2014) Methods for dilution antimicrobial susceptibility tests for bacteria that grow aerobically; NCCLS document M27-A, 15, 10, VA Medical Center, Tucson; Approved standard, 8th edn. CLSI M7-A9, USA
35. Dudová B, Hudecová D, Pokorný R, Mikulášová M, Palicová M, Segľa P, Melník M (2002) Folia Microbiol 47:225
36. Taniguchi L, de Fátima Faria B, Rosa RT, de Paula e Carvalho A, Gursky LC, Elifio-Esposito SL, Parahitiyawa N, Samaranayake LP, Rosa EAR (2009) J Microbiol Methods 78:171
37. Maron D, Ames B (1983) Mut Res 113:173